Direct Visualization of the EcoRII−DNA Triple Synaptic Complex by Atomic Force Microscopy†

Luda S. Shlyakhtenko,‡ Jamie Gilmore,‡ Alex Portillo,‡ Gintautas Tamulaitis,§ Virginijus Siksnys,§ and Yuri L. Lyubchenko*,‡

Department of Pharmaceutical Sciences, College of Pharmacy, University of Nebraska Medical Center, 986025 Nebraska Medical Center, Omaha, Nebraska 68198-6025, and Institute of Biotechnology, Graiciuno 8, LT-02241 Vilnius, Lithuania

Received June 6, 2007; Revised Manuscript Received August 20, 2007

ABSTRACT: Interactions between distantly separated DNA regions mediated by specialized proteins lead to the formation of synaptic protein−DNA complexes. This is a ubiquitous phenomenon which is critical in various genetic processes. Although such interactions typically occur between two sites, interactions among three specific DNA regions have been identified, and a corresponding model has been proposed. Atomic force microscopy was used to test this model for the EcoRII restriction enzyme and provide direct visualization and characterization of synaptic protein−DNA complexes involving three DNA binding sites. The complex appeared in the images as a two-loop structure, and the length measurements proved the site specificity of the protein in the complex. The protein volume measurements showed that an EcoRII dimer is the core of the three-site synaptosome. Other complexes were identified and analyzed. The protein volume data showed that the dimeric form of the protein is responsible for the formation of other types of synaptic complexes as well. The applications of these results to the mechanisms of the protein−DNA interactions are discussed.

Synaptic DNA−protein complexes (synaptosomes) are formed by DNA helices brought together and stabilized by a specialized protein or protein complexes. The formation of synaptic DNA−protein complexes is the key step of various genetic processes such as site-specific recombination, genome integration, excision, and inversion of specific DNA regions (*1*). In fact, the formation of a synaptic complex is a more general phenomenon that is not limited to site-specific recombination, insertion, and integration systems. There is a family of DNA restriction enzymes that require the formation of synaptic complexes for further site-specific DNA cleavage (*2*−*5*). In the majority of synaptic protein−DNA complexes, two DNA duplexes are involved in the synaptosome assembly. However, there are a number of reports indicating that more than two specific DNA regions can be involved in the formation of synaptic complexes. For example, a three-site synaptic complex is formed during Mu DNA transposition (*6*, *7*); in the His-mediated inversion reaction, a tripartite complex is formed when the His tetramer, holding hixL and hixR sites, interacts with the Fis dimer, which brings an enhancer site to the complex (*8*−*12*). These are complex multiprotein systems in which participation of multimers of the same protein (three MuA transposases for the Mu system) or more than two proteins (His-mediated invertasome) are involved. Very recent data from the Siksnys lab showed that efficient cleavage mediated by EcoRII restriction endonuclease also requires the formation of a synaptic complex involving three DNA recognition regions (*13*). EcoRII is a type IIE endonuclease, which cuts duplex DNA containing the sequence /CCWGG, with W being adenine (A) or thymine (T) (cleavage position indicated by the slash). Generally, EcoRII exists in solution as a dimer (∼90 kDa) that is capable of forming synaptic complexes via cooperative binding of two DNA regions (*14*). According to crystallographic data of EcoRII mutant R88A (*15*), the protein dimer is formed through the formation of helix bundles at the dimer interface, and both N- and C-domains participate in the dimerization. The model (*13*) suggests that the dimeric form of the enzyme is involved in the three-site synaptosome formation. To concertedly cleave the DNA strand, three sites need to be involved in the reaction, which includes the catalytic C-terminal domain and the two N-terminal domains. Exogenic oligonucleotides added to the reaction mixture increased the reaction velocity and changed the reaction pattern for EcoRII cleavage of one- or two-site plasmids but had little effect on the three-site plasmid (*13*).

To test this novel model for synaptic complex formation, we utilized AFM[1] to directly visualize the complexes formed by the EcoRII enzyme and DNA templates with a well-defined number and positioning of protein binding sites. EcoRII complexes have been previously visualized with electron microscopy, but formation of a three-site complex has not been reported (*16*). AFM has been successfully applied to various protein−DNA complexes (e.g., refs *17*−*26* and

† This work was supported by grants from NIH (GM 62235 to Y.L.L.), the INBRE/BRIN program (P20 RR16469 to J.G.), the UNMC undergraduate research program (A.P.), and Howard Hughes Medical Institute International Research Scholar Grant 55000336 (V.S.).

* To whom correspondence should be addressed: Department of Pharmaceutical Sciences, University of Nebraska Medical Center, 986025 Nebraska Medical Center, Omaha, NE 68198-6025. Phone: (402) 559-5320. Fax: (402) 559-9543. E-mail: ylyubchenko@unmc.edu.

‡ University of Nebraska Medical Center.

§ Institute of Biotechnology.

[1] Abbreviations: AFM, atomic force microscopy; APS, 1-(3-aminopropyl)silatrane.

10.1021/bi701123u CCC: $37.00
Published on Web 09/11/2007

references therein). Recent AFM experiments have been successful in the imaging of synaptosomes formed by the SfiI restriction enzyme (*27*, *28*). Moreover, these studies were instrumental in aiding our understanding of the arrangement of the DNA helices within the synaptosomes. Using the developed approaches, we were able to identify the formation of EcoRII triple synaptic complexes (TSC). Importantly, the protein volume measurements showed that the dimeric form of the protein is capable of holding together three DNA binding sites. Analysis of other EcoRII−DNA complexes allowed us to shed new light on the formation of different types of synaptic complexes.

MATERIALS AND METHODS

Proteins. The wild-type (wt) EcoRII protein and its EcoRII-N mutant were purified, and their concentrations were determined by the Bradford assay as described in refs *13* and *29*.

EcoRII-C was obtained by thermolysin digestion of the Y41A mutant of EcoRII which possesses low cleavage activity (*30*). One milligram of Y41A EcoRII was digested for 3 h at 25 °C with 0.1 mg of thermolysin (Sigma) in a final volume of 2 mL as described in ref *29*. The solution was loaded onto a HiTrap Heparin column (Amersham Pharmacia Biotech) pre-equilibrated with 20 mM Tris-HCl (pH 8.0 at 25 °C), 0.1 M KCl, 1 mM EDTA, 7 mM 2-mercaptoethanol, and 10% glycerol, and protein was eluted from the column with a linear KCl gradient. The fractions were analyzed with a λ DNA cleavage assay that monitored the EcoRII-C activity which is unleashed during the proteolysis (*31*) and SDS−PAGE. Fractions containing EcoRII-C were pooled, dialyzed against 10 mM Tris-HCl (pH 7.4 at 25 °C), 0.2 M KCl, 1 mM EDTA, 1 mM DTT, and 50% glycerol, and stored at −20 °C. SDS−PAGE analysis revealed that the sample contained >95% of the C-terminal domain and showed no traces of the full-length protein. The concentration of EcoRII-C was determined by measuring the absorbance at 280 nm using an extinction coefficient of 43 240 M^{-1} cm^{-1} calculated for the dimer by the ProtParam tool (http://www.expasy.ch/).

All concentrations of wt EcoRII and EcoRII-C are indicated in terms of dimer and EcoRII-N in terms of monomer. Restriction endonuclease MvaI was purchased from Fermentas (Vilnius, Lithuania).

Preparation of DNA Fragments. Two different DNA fragment designs were examined in this study, the PCR1 fragment, which contains one recognition site, and the PCR3 fragment, which contains three recognition sites. The fragments were obtained by PCR amplification of selected regions from the pBluescript IIKS(+) plasmid (*32*). PCR primers were designed to amplify a defined region of interest to include the correct number of EcoRII restriction sites. The restriction sites are denoted A1, T, and A2 (Figure 1A). The letters indicate the central base in the EcoRII recognition site, CCWGG, that is found on the leading strand. The PCR1 fragment is 205 bp long, with 5 bp recognition site A2 in the center and 100 bp flanks on either side (Figure 5D). The 810 bp PCR3 fragment was obtained by PCR to include all three restriction sites. The design of the PCR3 fragment consists of 100 bp arms, with segments between each 5 bp recognition site, which are 312 and 283 bp long. A1 and A2 are two outer sites, with the T site between the two A sites.

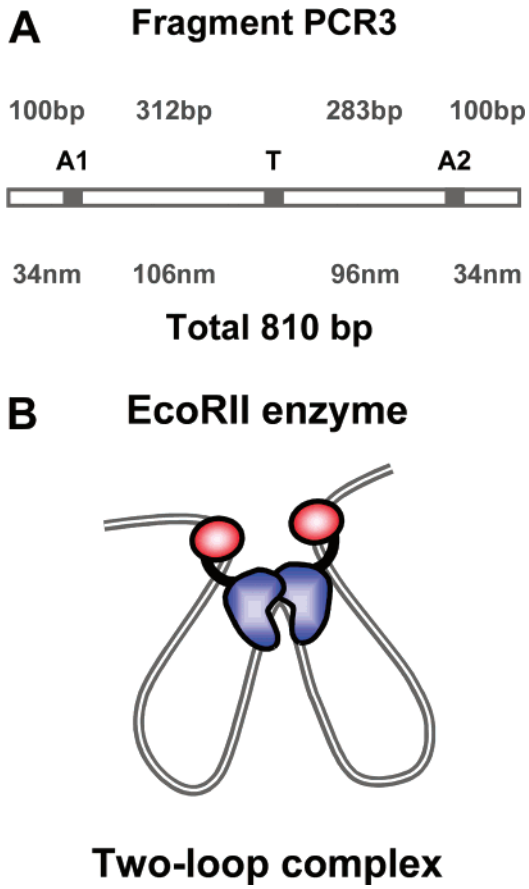

FIGURE 1: PCR3 fragment. (A) Linear fragment containing three EcoRII recognition sites (A1, T, and A2) indicated in base pairs and nanometers. (B) Model for the two-loop complex of EcoRII with the PCR3 fragment bound at all three sites.

The PCR products were precipitated with 2-propanol dissolved in deionized water and loaded onto a 2% agarose gel. The gel was run in TAE [40 mM Tris-acetate (pH 8.0 at 25 °C) and 1 mM EDTA] buffer and stained with ethidium bromide. The fragments were cut and purified from the gel using the QIAquick gel extraction kit (Qiagen, Hilden, Germany) and eluted with 10 mM Tris-HCl (pH 7.8 at 25 °C) buffer. The concentrations of DNA fragments were determined by measuring the absorbance at 260 nm. The correct positioning of the restriction sites was verified using the MvaI restriction endonuclease, which recognizes the same restriction site (CCWGG) yet does not require binding to multiple sites (*33*), thus cleaving with a higher efficiency. The digestion products were run on an agarose gel, which indeed showed bands corresponding to expected lengths (Figure S2B, Supporting Information).

Preparation of EcoRII−DNA Complexes. The conditions for the binding reaction for the wild-type and mutant EcoRII protein with DNA fragments were chosen on the basis of the gel shift assay data shown in Figures S5−S7 (Supporting Information). Gel shift data for the wild-type EcoRII protein were performed either in the presence of EDTA or in the presence of Ca^{2+} (Figure S5, Supporting Information). Both conditions were tested. For the EcoRII-C mutant, the binding reaction was conducted in the presence of Ca^{2+} (Figure S6, Supporting Information), and for the EcoRII-N mutant, EDTA was added instead (Figure S7, Supporting Information). A detailed protocol of the conditions for the complex formation for each individual protein is given below.

Binding reactions for wt EcoRII with the PCR3 fragment were carried out with a protein:DNA ratio of 2−3 protein dimers per DNA fragment (0.6−1 protein dimer per recognition site). To allow enzyme binding but prevent cleavage, buffer containing Ca^{2+} was used instead of Mg^{2+}. Reaction mixtures (10 μL total) contained 10−100 nM PCR3 fragment, 20−200 nM EcoRII protein, 40 mM HEPES (pH 8.4), and 5 mM $CaCl_2$. Binding reactions for the wt EcoRII protein with the PCR1 fragment were performed at a 1:1 protein:DNA ratio. The final reaction mixture contained 209 nM EcoRII, 205 nM PCR1, 40 mM HEPES (pH 8.4), and 5 mM $CaCl_2$.

Reaction mixtures for the EcoRII mutants were prepared with different protein:DNA ratios and buffer conditions. Binding reactions for the EcoRII-N mutant with the PCR3 fragment were performed with a protein:DNA ratio of 26:1. The final reaction mixture contained 107 nM PCR3, 2844 nM EcoRII-N, 0.1 mM EDTA, and 10 mM HEPES (pH 8.4). Binding reactions for the EcoRII-C mutant with the PCR3 fragment were performed with a protein:DNA ratio of 435:1 to observe binding. The final reaction mixture contained 15.3 nM PCR3 fragment, 6700 nM EcoRII-C, 40 mM HEPES (pH 8.4), and 5 mM $CaCl_2$.

All reaction mixtures were incubated at room temperature for 15 min and then fixed with 0.5% glutaraldehyde for 10 min. The fixation reaction was stopped by adding 1−2 μL of 2 M Tris-HCl (pH 7.1). After completion of the fixation step, the complexes were purified using Montage PCR filter units (Millipore Corp., Bedford, MA). To purify the samples, 300 μL of 10 mM HEPES (pH 7.4) was spin-filtered through them. The final samples were resuspended in 10 μL of 10 mM HEPES (pH 7.4). Appropriate dilutions were made before the deposition of the samples onto mica to provide an even spread of DNA on the surface for AFM imaging.

AFM. Freshly cleaved muscovite ruby mica was incubated in a mixture of a 1-(3-aminopropyl)silatrane (APS) solution for 30 min to prepare APS-mica, as described previously (*22*, *24*, *25*, *27*, *28*, *34*). The sample droplets (5 μL) were deposited on APS-mica for 2 min, then washed with deionized water, and dried with argon. The mica was attached to a metal disc with double-stick tape for imaging. Images were acquired in tapping mode in air and using a Multimode SPM Nanoscope IV system (Veeco/Digital Instruments, Santa Barbara, CA). Silicon-etched tapping mode probes (TESP7; Veeco/Digital Instruments) were used. They had nominal spring constants of ∼42 N/m and a resonant frequency of ∼320 Hz.

Data Analysis. For each type of EcoRII−DNA complex formed, data were obtained for the length of the DNA fragments, the volume of the protein, and the yields of the various complexes using Femtoscan Online (Advanced Technologies Center, Moscow, Russia). Contour length measurements of the DNA molecule were made by tracing the image of the DNA backbone using the curve tool and obtaining the readout from Femtoscan.

The protein volume measurements were performed using the section tool from Femtoscan. Perpendicular cross sections were made to record the width in two dimensions. The height (h) of the protein was measured by the difference in the intensity of the protein compared to the background noise. The widths were measured at half of the maximal protein height. The volume (V) of the protein was determined using eq 1 (*35*):

$$V = \frac{h\pi}{6}\left(\frac{3ab}{4} + h^2\right) \quad (1)$$

Taking into account the fact that the three-dimensionality of the synaptic complex formed by a large protein dimer could have different projections on a plane, one should expect some variation of the protein volume calculated from this approximation. The volume of the protein was converted into mass in kilodaltons by dividing by a coefficient of 1.92, obtained from the comparison with the volume for SfiI restriction endonuclease (*27*, *28*).

The data for the length and volume measurements were analyzed using Origin 6.0 (Originlab, Northampton, MA). The histograms were approximated by Gaussian curves, and the maximum of the distribution determined the most probable value for the event.

RESULTS

Visualization and Characterization of the Two-Loop EcoRII−DNA Complexes. The main goal of this study was to test the three-site binding model of restriction endonuclease EcoRII bound to DNA. To accomplish this goal, a template containing three sites (PCR3) was designed (Figure 1A). This DNA molecule has three EcoRII recognition sites placed almost symmetrically within the molecule, but not quite. The formation of a TSC mediated by the enzyme binding should lead to the formation of a two-loop molecule, with approximately equally sized loops (Figure 1B). The distances between sites A1 and T, as well as between A2 and T, were made approximately twice the DNA persistence length (312 and 283 bp, respectively) to ease potential problems with loop formation due to the relatively high rigidity of double-stranded DNA (e.g. refs *26* and *36*).

The PCR3 fragment and wt EcoRII protein were mixed to form a complex as described in Materials and Methods. The Mg^{2+} cations were replaced with Ca^{2+} cations to prevent DNA cleavage, and the complexes were cross-linked with glutaraldehyde. Figure 2A shows an AFM image of the complex with a two-loop complex in the middle of the image. A zoomed image of this two-loop complex is shown in the inset (i). A collage of several two-loop complexes is shown in Figure 2B−F. These are molecules of qualitatively similar morphologies: two loops of relatively similar sizes and short linear arms.

We measured the lengths of loops and of linear arms for the molecules to test whether the complexes are formed by specific binding of the enzyme to the cognate recognition sites on the DNA fragment. The results for the measurements of arms, loops, and entire contour lengths of the two-loop complexes are shown as histograms in panels A−C of Figure 3, respectively. Note that the histogram for the loop sizes contains the combined data for both loops, as their sizes were too similar to distinguish between them, so the data appear as a one-peak histogram. The expected sizes for corresponding distances for DNA contour length and the length between sites A1 and T, as well as between A2 and T (loops), and also the ends of the molecules, were calculated assuming a B-conformation of the DNA duplex. It is seen (Figure 1A) that the anticipated values are very close to the measured

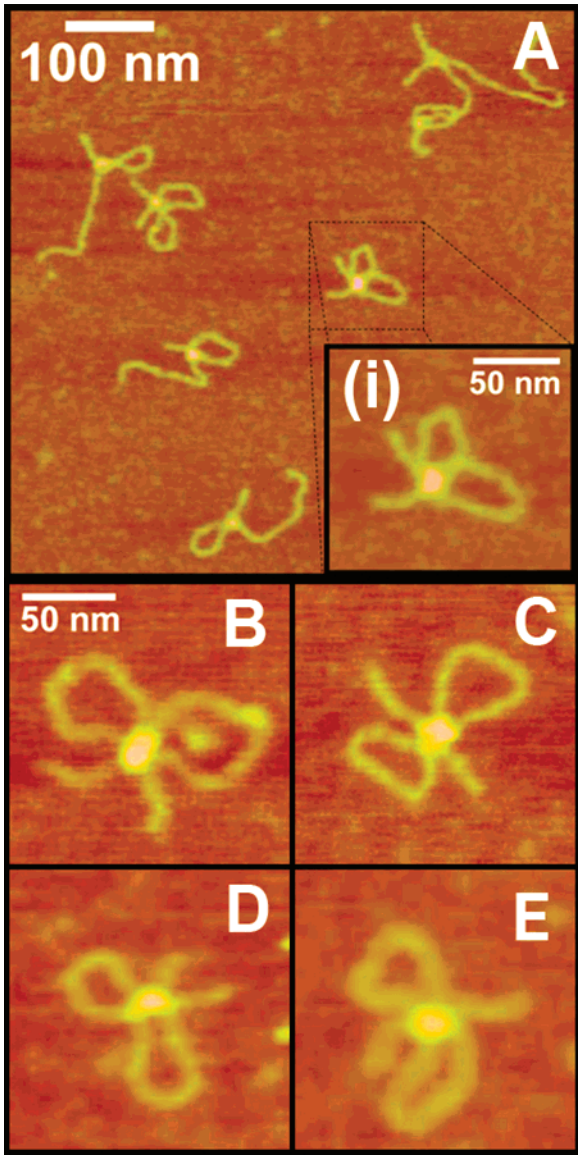

FIGURE 2: AFM images of the EcoRII−DNA complexes. (A) Large scan with various complexes. A two-loop complex in the middle of the scan is boxed. A zoomed image of this two-loop complex is shown as an inset (i). (B−E) Gallery of AFM images for two-loop DNA protein complexes, where the size of the bar (50 nm) applies to all images.

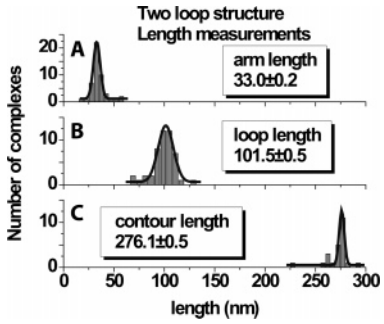

FIGURE 3: Histograms of measured length values for the EcoRII−PCR3 two-loop structures: arm length (A), loop length (B), and contour length (C). The lengths correspond to expected values, which are 34 nm (A), 97.9 and 107.8 nm (B), and 278.8 nm (C).

ones. Thus, the data obtained confirm that the two-loop structures are specific three-site complexes formed by the enzyme. Note that no such looped complexes were observed for control samples with no protein added (data not shown).

We also performed the measurements of the protein volume to evaluate the molecular mass of the protein and thus to determine the stoichiometry of the protein within the complex. The data for the volume measurements for two-loop complexes are shown as a histogram in Figure S1 (Supporting Information). The volume data were converted into the molecular mass and vice versa using the conversion coefficient as described in Materials and Methods. From these conversions, the anticipated volume of an EcoRII dimer is 175.1 nm^3. This value is close to the mean value of 167 nm^3 for the volume of the protein obtained from the histogram in Figure S1 (Supporting Information). Thus, the AFM data show that the two-loop complexes are formed by EcoRII and that dimerization of the protein is sufficient for that.

Characterization of Other Types of EcoRII−PCR3 Complexes. In addition to two-loop complexes, the enzyme forms other types of complexes with the same DNA template. Additional EcoRII complexes with the PCR3 fragment were identified and divided into four major groups, as shown in Figure 4. The first group (Figure 4A) comprises the synaptic complexes, including the small loop and large loop structures. Insets i and ii show representative AFM images of these structures. The small loop can be formed by the protein binding at the central recognition site (T, Figure 1) and one of the outer sites (A1 or A2, Figure 1), and the big loop can be formed by protein binding at the two outer sites (A1 and A2, Figure 1). Three other complexes (Figures 4B−D) are observed on a linear DNA template with different numbers of protein blobs per molecule: one-site occupied fragments (B), two-site occupied fragments (C), and three-site occupied fragments (D). These complexes were analyzed in a manner similar to that used for the two-loop complexes, and the results of the analysis given in Table 1 confirm that these are site-specific complexes.

We also characterized the stoichiometry of the complexes by performing protein volume measurements. The volume measurement results for the synaptic looped complexes are shown in Figure 4A. The volumes for all looped complexes are centered around the value of 180 nm^3 (or a molecular mass of 93.8 kDa) corresponding to the dimer state of the enzyme. However, when the protein is found associated with one single site, the histogram for the protein volume shows a bimodal distribution (Figure 4B−D), corresponding to the values for either a monomer or a dimer.

The yields for each type of PCR3−EcoRII complex vary. The two-loop complexes were found to have a yield of 1.7%. The yield of the complex with a big loop is 2 times higher (3.2%), but the small loop complexes are the most abundant type of complex among all specific complexes (52.2%). Interactions with a single recognition site were also observed in substantial yields (33.5%). Other types of nonlooped complexes (two sites and three sites) constituted 9.3%.

Characterization of EcoRII−PCR1 Complexes. We analyzed complexes of EcoRII with a one-site DNA fragment, PCR1. Both linear and synaptic complexes formed by two DNA molecules (*trans* X-type complexes) were identified and characterized (Figure 5). The most abundant were the linear complexes with one protein bound to the DNA template (64.6%; Figure 5A, molecules 2 and 3). The

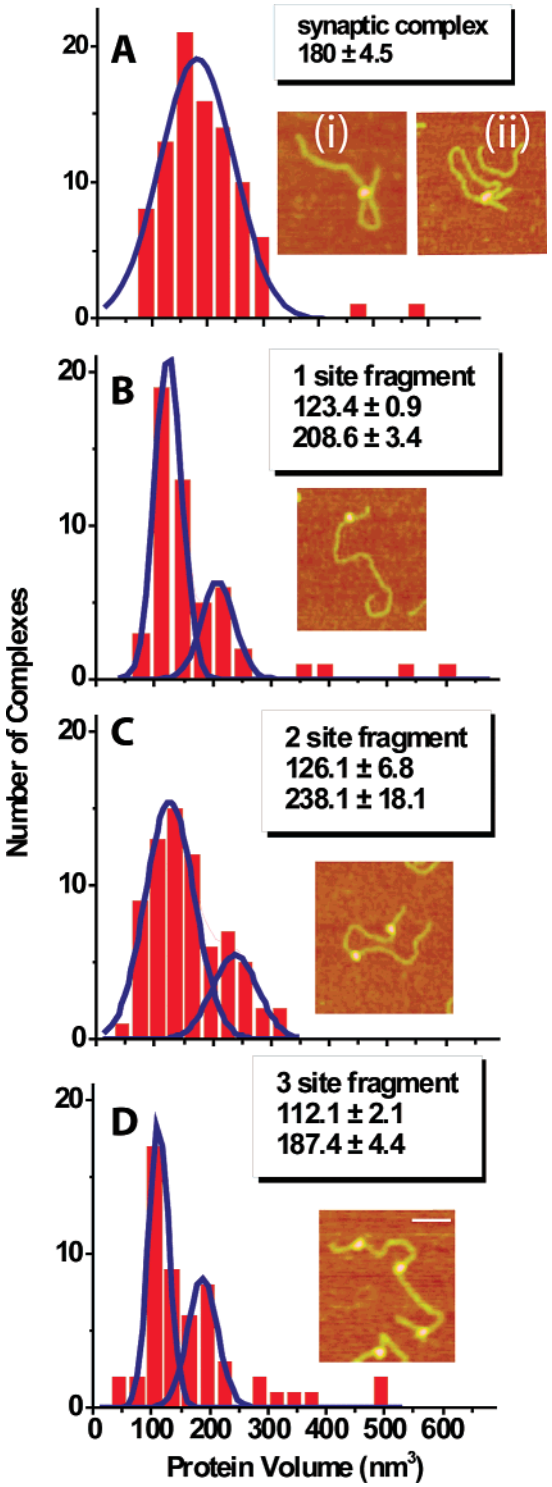

FIGURE 4: AFM data for different types of complexes of EcoRII with the PCR3 template. (A) Looped synaptic complexes. Inset images (i and ii) illustrate small loop and large loop synaptic complexes, respectively. (B) One-site complexes. (C) Two-site complexes. (D) Complexes with three sites occupied (PCR3−EcoRII). Representative AFM images for each type of complex are shown next to the corresponding histograms.

synaptic X-type complexes (Figure 5A, molecule 1) had a yield of 12.1%. The length measurement for the shortest arm of the linear complex (30.1 nm) and the length measurement for all four arms of the synaptic complex (33.4 nm) corresponded to the expected values for specific binding (34 nm).

We measured the protein volume to estimate the protein stoichiometry for the PCR1 fragment. The histogram (Figure 5B) for the synaptic complex volume is approximated with one Gaussian with a maximum of 200.1 nm^3 (104.2 kDa) which is close to the expected value for a dimer (175.2 nm^3). The histogram for complexes on the linear DNA fragment (Figure 5C) is broad and approximated with two Gaussians with maxima at 88.9 and 182 nm^3, corresponding to both monomeric and dimeric forms of the enzyme. Note that free protein appears as spherical blobs with the mean volume value (185.6 ± 5.8. nm^3) corresponding to the protein dimer.

Characterization of the DNA−EcoRII Mutant Complex. To gain additional insight into the mechanism of formation of the EcoRII−DNA complexes, we conducted experiments with the PCR3 fragments using two mutant forms of the enzyme. The N-terminal and C-terminal mutants are truncated forms of the EcoRII protein. The N-terminal mutant contains the N-terminal domain (EcoRII-N), and the C-terminal mutant contains the C-terminal domain (EcoRII-C) (*13*). Complexes of the PCR3 fragment with both deletion mutants were obtained, imaged, and analyzed. The results for the arm length measurements for the complexes having only one site occupied are shown in Figure 6. The expected values for the arm lengths of 100 bp (34 nm) and 388 bp (131.92 nm) or 417 bp (141.78 nm) corresponded well to the major peaks for both types of mutants, suggesting that the both mutants recognize specific regions on the DNA template. However, there were a large number of events that fell outside of the peaks with the EcoRII-C mutant, suggesting binding at noncognate sites. Few loops were identified for the EcoRII-N mutant (11 loops of a total of 197 complexes analyzed, or 5.59%). The position of the protein on the loop varied greatly, with the length of the shortest arm around 44.1 nm, and a mean loop size of ~135 nm. These values do not correlate well with the expected values for loop formation via binding to specific regions and most likely result from aggregation of the protein bound to the noncognate sites.

DISCUSSION

Three-Site Synaptic Complex. The results obtained show that EcoRII is capable of bringing together three recognition sites to form a TSC, as well as forming typical synaptic complexes requiring the interaction of two DNA recognition sites. Importantly, the dimerization of the protein is sufficient for accomplishing all of these binding modes. These findings are fully in line with the model proposed earlier which presumes that three-site binding is required for efficient and coordinated cleavage of the duplex, which includes one catalytic C-terminal domain and two N-terminal DNA binding domains to bridge three DNA recognition sites (*13*). The visualization of the three-site complex is the first direct justification of the model.

The low yield of TSC complexes (ca. 1.7%) is not surprising as it is comparable with the low yield of the large one-loop complex (3.2%). A surprising finding is that the yield of small loop complexes occurs at a percentage of 52.2% and is the highest yield among all types of possible EcoRII−PCR3 complexes. The probability of loop formation of various sizes can contribute to the yield of synaptic complexes (*37*, *38*). Such probability is quantitatively

Table 1: Measured Length Values for wt EcoRII−PCR3 Complexes[a]

complex type	contour length	arm length	loop length	segment length
small loop ($N = 80$)	279.2 ± 0.5	33.0 ± 0.3, 135.6 ± 0.4	106.7 ± 0.3	
big loop ($N = 43$)	279.2 ± 1.1	32.6 ± 0.3	207.0 ± 1.2	
double loop ($N = 22$)	276.1 ± 0.5	33.0 ± 0.2	101.5 ± 0.5	
one site occupied ($N = 52$)	277.8 ± 0.9	30.7 ± 0.4, 134.6 ± 0.7		
two sites occupied ($N = 36$)	276.3 ± 0.5	31.9 ± 0.3, 137.0 ± 0.5		106.0 ± 0.3, 208.0 ± 0.1
three sites occupied ($N = 18$)	276 ± 0.5	31.3 ± 0.3		103.7 ± 0.4

[a] All values corresponded well to the expected values. Multiple peaks on the histogram could not be distinguished for values that were close together, resulting in a number that fell between the two expected values. Standard errors of the mean from the Gaussian fit are indicated for each value.

characterized by the DNA cyclization *J*-factor (e.g., refs *38*−*40*). Using the table for *J*-factors calculated for a large set of DNA fragments varied between 200 and 800 bp (kindly provided by A. Vologodskii), we obtained a rather low variability of *J*-factors in the range between ∼300 and ∼600 bp. Specifically, the smallest value of the *J*-factor (27.4 nM) corresponds to the 283 bp distance; a slightly higher value (40 nM) is obtained for the 312 bp distance, and the highest *J*-factor value (63.5 nM) is predicted for 600 bp distances. On the basis of these estimates for *J*-factors, we would anticipate the highest yield of looped complexes for the large loop with slightly lower yields for the small loops. The data obtained for yields for large and small loops are just the opposite, 3.2% of complexes with the large loop compared to 52.2% of the formation of small loops, suggesting that the probability of DNA cyclization does not explain the observed effect in the loop formation. Note that the difference between the loops with 283 and 312 bp cannot be distinguished by the AFM length measurements, so we are unable to partition the 52.2% yield between these two loops. However, we have to take into account the inherent curvature of the DNA segments. Theoretical *J*-factor values depend on the sequence and can vary over a broad range (e.g., refs *39* and *41*−*43* and references therein). Motifs such as curved A-tracts are considered as the major factors influencing the path of the double helix and the *J*-factor values. Such motifs can be found in the 810 DNA template (Figure S2A of the Supporting Information). Experimentally, the inherent curvature of DNA can be characterized by gel electrophoresis, so the phased A-tracts can lead to curving of the DNA path and thus a decrease in the electrophoretic DNA mobility (e.g., ref *44*). To verify whether the DNA segments between internal sites (A1 and T and T and A2) have an elevated inherent curvature, we measured the electrophoretic mobility of restriction fragments obtained after MvaI digestion. Figure S2B of the Supporting Information shows that the electrophoretically determined lengths of the A1−T and T−A2 fragments (293 and 322 bp, respectively) are very close to their expected lengths (283 and 312 bp, respectively). These results suggest that the fragments or A1−T and T−A2 segments are not intrinsically curved. Therefore, we conclude that the contribution of loop size to the efficiency of the formation of synaptic complexes is not that essential. We should take into account the fact that the EcoRII recognition sequence is 5′-CCWGG-3′, where W can be either adenine (A) or thymine (T), and large and small loops are formed via the use of different sequences (Figure 1). The difference in the sequences of the sites involved in the formation of large and small loops is another potential explanation for the observed non-even looping effect. This hypothesis is in line with the photo-cross-linking experiments, which demonstrate that the N-terminal domain binding to the recognition site is asymmetric (*30*).

Additional insights into the EcoRII−DNA interactions come from the protein volume measurements of various complexes. The data show that the dimeric form of the enzyme is required for the synaptic and three-site complex formation, but the monomeric form also provides stable one-site binding. On the other hand, the protein dimers are found at individual binding sites as well. According to previously published data (*13*, *14*, *29*), EcoRII exists in solution as a dimer, so the appearance of the monomeric form in the complex could indicate protein−protein interactions that are weaker than protein−DNA interactions and reflect the dynamic nature of the EcoRII−DNA complex. Indeed, if the protein binds DNA as a dimer and then dissociates, one should expect to see some partially dissociated complexes as intermediates. Note that the intermediate states of the complex can be detected with AFM. Figure S3 shows a set of such intermediate complexes with a monomer bound to each individual site for different synaptic complexes: two-loop complexes (A), small loop complexes (B and C), and big loop complexes (D). Such synaptic complexes were not counted and considered to be not fully formed complexes. In the case of nonsynaptic complexes (one, two, or three sites occupied by protein), it is impossible to distinguish between fully formed and partially dissociated complexes, and that could explain the coexistence of both monomer and dimer binding modes.

The model for the formation of the TSC, as proposed previously (*13*) (see Figure 1B), assumes that DNA helices are severely bent within the complex. DNA is a rather stiff polymer (e.g. refs *26* and *36*), so bent DNA is an unfavorable conformation but can be compensated by the interaction with the protein. However, tracing of the molecules in two-loop complexes showed that the model with severe bends can be replaced with an alternative one in which the strands within the synaptosome are crossed, allowing fewer bends. Figure S4 shows dotted lines for a path where DNA strands bend (A) and cross (B). Both types of traces fit to the expected contour length of the fragment. However, available DNA templates do not allow one to unambiguously distinguish between these models. Designs similar to ones used in our paper about the AFM analysis of synaptic SfiI−DNA synaptosomes would provide the answer (*28*).

The protein−DNA synaptosomes are key intermediates for the various site-specific DNA interactions, and the traditional model assumes the participation of two DNA sites in the formation of the complex. This study shows that three sites can be involved in the formation of a complex stabilized

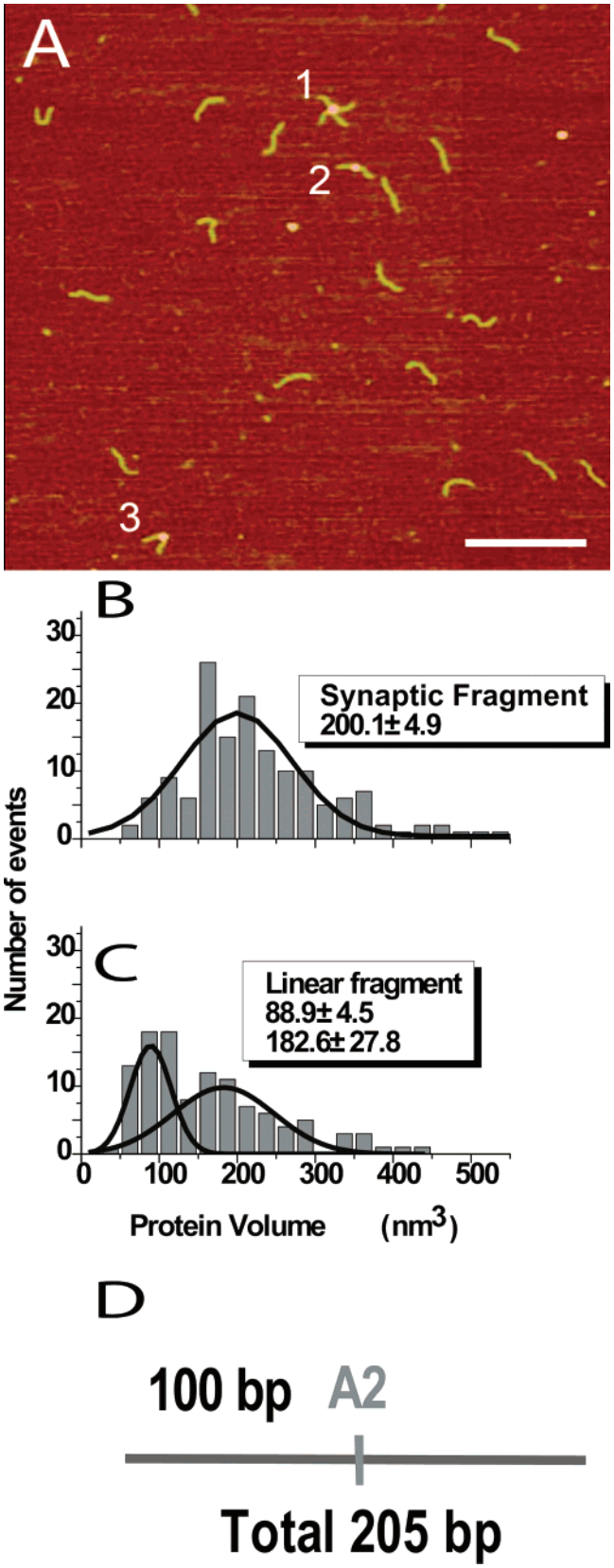

FIGURE 5: AFM data for EcoRII−PCR1 complexes. (A) AFM images of PCR1−EcoRII complexes: synaptic complex (1) and single-site occupied complexes (2 and 3). The bar equals 200 nm. (B) Volume distribution for the synaptic complex. The peak value of 200.1 nm^3 corresponds to a molecular mass of 104.2 kDa. (C) Volume distribution for a single-site occupied complex. The peak values of 88.9 and 182.6 nm^3 correspond to molecular masses of 46.3 and 95.1 kDa, respectively. (D) Schematic presentation of the PCR1 fragment.

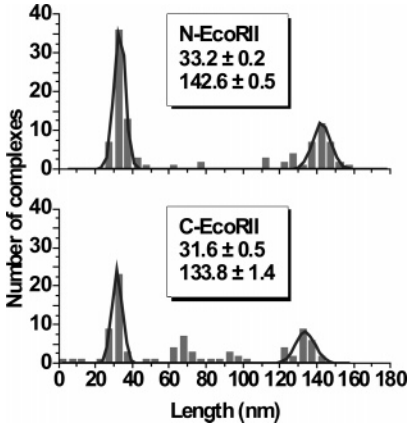

FIGURE 6: Histograms of the EcoRII mutants' short arm length distributions: N-terminal mutant (A) and C-terminal mutant (B). Both histograms have peaks corresponding to the expected length values of 34 and 132 nm, respectively. EcoRII-C appears to bind with much less specificity than EcoRII-N.

by one protein dimer. However, the interactions requiring three sites are not that rare. Three sites can be brought together, but typically, it requires the participation of at least two proteins. For example, a three-site synaptic complex is formed during Mu DNA transposition (*6*, *7*). In this insertion process, the transpositional enhancer is actively involved in direct interaction with the Mu left and right ends, leading to the formation of a three-site synaptic (LER) complex. A similar tripartite interaction including the involvement of two different site-specific DNA-binding proteins provides the His-mediated inversion reaction (*8*−*12*). In this system, the invertasome tripartite complex is formed by the His tetramers holding hixL and hixR sites and Fis dimer, which brings the enhancer to the complex. However, the three-site interaction can be formed transiently in the process of searching for specific sites via sliding of nonspecifically formed synaptic complexes. This model was suggested by Cherepanov et al. (*45*) on the basis of electron microscopy analysis of the integration of human immunodeficiency virus type 1 (HIV-1) cDNA by the HIV-1 integrase. The loop sizes of the two-loop complexes varied over a broad range, leading the authors to hypothesize that two-loop or three-site synaptic complexes are transient states in the process of finding the specific site by protein sliding along DNA. The mechanisms whereby the protein finds the target on the DNA substrate are widely discussed in the literature. Sliding is one of the mechanisms that provides an efficient search of specific sites leading to the formation of productive synaptic complexes (*46*). The search process can be accelerated substantially if the site transfer mechanism is involved (*46*). If the protein(s) holds two DNA sites, and another one is captured via the strand transfer process, the intermediate state would be a TSC complex. The binding of the third site can be prompted in a manner similar to one observed for the EcoRII enzyme, in which the DNA binding site is formed by the interaction of the C-termini during protein dimerization. Thus, the TSC conformation of the synaptosome can exist transiently, facilitating the site search function to the synaptosome. The use of single-molecule techniques, including time-lapse AFM, capable of detecting transient states of molecules and their complexes [e.g., the recent paper (*47*)], will be instrumental in unraveling the site search mechanisms and the role of formation of the TSC complex in particular.

Further studies of the dynamics of three-site EcoRII−DNA synaptic complexes would shed new light on the mechanisms by which proteins search for their specific binding site.

ACKNOWLEDGMENT

We thank A. Vologodskii for providing us with his detailed table about the length dependence of the DNA cyclization efficiency and Monika Reuter (Institute of Virology at Humboldt University, Berlin, Germany) for the clones of wt EcoRII, the N-terminal domain, and the Y41A mutant.

SUPPORTING INFORMATION AVAILABLE

Procedures for the preparation and characterization of proteins, major features of the sequences of the DNA templates used in the paper, and additional data for the AFM characterization of EcoRII−DNA complexes. This material is available free of charge via the Internet at http://pubs.acs.org.

REFERENCES

1. Grindley, N. D., Whiteson, K. L., and Rice, P. A. (2006) Mechanisms of Site-Specific Recombination, *Annu. Rev. Biochem. 75*, 567−605.
2. Bilcock, D. T., and Halford, S. E. (1999) DNA restriction dependent on two recognition sites: Activities of the SfiI restriction-modification system in *Escherichia coli*, *Mol. Microbiol. 31*, 1243−1254.
3. Embleton, M. L., Siksnys, V., and Halford, S. E. (2001) DNA cleavage reactions by type II restriction enzymes that require two copies of their recognition sites, *J. Mol. Biol. 311*, 503−514.
4. Bath, A. J., Milsom, S. E., Gormley, N. A., and Halford, S. E. (2002) Many type IIs restriction endonucleases interact with two recognition sites before cleaving DNA, *J. Biol. Chem. 277*, 4024−4033.
5. Gormley, N. A., Hillberg, A. L., and Halford, S. E. (2002) The type IIs restriction endonuclease BspMI is a tetramer that acts concertedly at two copies of an asymmetric DNA sequence, *J. Biol. Chem. 277*, 4034−4041.
6. Watson, M. A., and Chaconas, G. (1996) Three-site synapsis during Mu DNA transposition: A critical intermediate preceding engagement of the active site, *Cell 85*, 435−445.
7. Kobryn, K., Watson, M. A., Allison, R. G., and Chaconas, G. (2002) The Mu three-site synapse: A strained assembly platform in which delivery of the L1 transposase binding site triggers catalytic commitment, *Mol. Cell 10*, 659−669.
8. Merickel, S. K., Haykinson, M. J., and Johnson, R. C. (1998) Communication between Hin recombinase and Fis regulatory subunits during coordinate activation of Hin-catalyzed site-specific DNA inversion, *Genes Dev. 12*, 2803−2816.
9. Heichman, K. A., Moskowitz, I. P., and Johnson, R. C. (1991) Configuration of DNA strands and mechanism of strand exchange in the Hin invertasome as revealed by analysis of recombinant knots, *Genes Dev. 5*, 1622−1634.
10. Heichman, K. A., and Johnson, R. C. (1990) The Hin invertasome: Protein-mediated joining of distant recombination sites at the enhancer, *Science 249*, 511−517.
11. Merickel, S. K., and Johnson, R. C. (2004) Topological analysis of Hin-catalysed DNA recombination in vivo and in vitro, *Mol. Microbiol. 51*, 1143−1154.
12. Merickel, S. K., Sanders, E. R., Vazquez-Ibar, J. L., and Johnson, R. C. (2002) Subunit exchange and the role of dimer flexibility in DNA binding by the Fis protein, *Biochemistry 41*, 5788−5798.
13. Tamulaitis, G., Sasnauskas, G., Mucke, M., and Siksnys, V. (2006) Simultaneous binding of three recognition sites is necessary for a concerted plasmid DNA cleavage by EcoRII restriction endonuclease, *J. Mol. Biol. 358*, 406−419.
14. Reuter, M., Kupper, D., Meisel, A., Schroeder, C., and Kruger, D. H. (1998) Cooperative binding properties of restriction endonuclease EcoRII with DNA recognition sites, *J. Biol. Chem. 273*, 8294−8300.
15. Zhou, X. E., Wang, Y., Reuter, M., Mucke, M., Kruger, D. H., Meehan, E. J., and Chen, L. (2004) Crystal structure of type IIE restriction endonuclease EcoRII reveals an autoinhibition mechanism by a novel effector-binding fold, *J. Mol. Biol. 335*, 307−319.
16. Mucke, M., Lurz, R., Mackeldanz, P., Behlke, J., Kruger, D. H., and Reuter, M. (2000) Imaging DNA loops induced by restriction endonuclease EcoRII. A single amino acid substitution uncouples target recognition from cooperative DNA interaction and cleavage, *J. Biol. Chem. 275*, 30631−30637.
17. Lyubchenko, Y. L., Blankenship, R. E., Gall, A. A., Lindsay, S. M., Thiemann, O., Simpson, L., and Shlyakhtenko, L. S. (1996) Atomic force microscopy of DNA, nucleoproteins and cellular complexes: The use of functionalized substrates, *Scanning Microsc., Suppl. 10*, 97−107.
18. Herbert, A., Schade, M., Lowenhaupt, K., Alfken, J., Schwartz, T., Shlyakhtenko, L. S., Lyubchenko, Y. L., and Rich, A. (1998) The Zα domain from human ADAR1 binds to the Z-DNA conformer of many different sequences, *Nucleic Acids Res. 26*, 3486−3493.
19. Lyubchenko, Y. L., Gall, A. A., and Shlyakhtenko, L. S. (2001) Atomic force microscopy of DNA and protein-DNA complexes using functionalized mica substrates, *Methods Mol. Biol. 148*, 569−578.
20. Bash, R. C., Yodh, J., Lyubchenko, Y., Woodbury, N., and Lohr, D. (2001) Population analysis of subsaturated 172-12 nucleosomal arrays by atomic force microscopy detects nonrandom behavior that is favored by histone acetylation and short repeat length, *J. Biol. Chem. 276*, 48362−48370.
21. Yodh, J. G., Woodbury, N., Shlyakhtenko, L. S., Lyubchenko, Y. L., and Lohr, D. (2002) Mapping nucleosome locations on the 208-12 by AFM provides clear evidence for cooperativity in array occupation, *Biochemistry 41*, 3565−3574.
22. Virnik, K., Lyubchenko, Y. L., Karymov, M. A., Dahlgren, P., Tolstorukov, M. Y., Semsey, S., Zhurkin, V. B., and Adhya, S. (2003) "Antiparallel" DNA loop in gal repressosome visualized by atomic force microscopy, *J. Mol. Biol. 334*, 53−63.
23. Lushnikov, A. Y., Brown, B. A., II, Oussatcheva, E. A., Potaman, V. N., Sinden, R. R., and Lyubchenko, Y. L. (2004) Interaction of the Zα domain of human ADAR1 with a negatively supercoiled plasmid visualized by atomic force microscopy, *Nucleic Acids Res. 32*, 4704−4712.
24. Potaman, V. N., Shlyakhtenko, L. S., Oussatcheva, E. A., Lyubchenko, Y. L., and Soldatenkov, V. A. (2005) Specific binding of poly(ADP-ribose) polymerase-1 to cruciform hairpins, *J. Mol. Biol. 348*, 609−615.
25. Lonskaya, I., Potaman, V. N., Shlyakhtenko, L. S., Oussatcheva, E. A., Lyubchenko, Y. L., and Soldatenkov, V. A. (2005) Regulation of poly(ADP-ribose) polymerase-1 by DNA structure-specific binding, *J. Biol. Chem. 280*, 17076−17083.
26. Lyubchenko, Y. L. (2004) DNA structure and dynamics: An atomic force microscopy study, *Cell Biochem. Biophys. 41*, 75−98.
27. Lushnikov, A. Y., Potaman, V. N., and Lyubchenko, Y. L. (2006) Site-specific labeling of supercoiled DNA, *Nucleic Acids Res. 34*, e111.
28. Lushnikov, A. Y., Potaman, V. N., Oussatcheva, E. A., Sinden, R. R., and Lyubchenko, Y. L. (2006) DNA Strand Arrangement within the SfiI-DNA Complex: Atomic Force Microscopy Analysis, *Biochemistry 45*, 152−158.
29. Tamulaitis, G., Mucke, M., and Siksnys, V. (2006) Biochemical and mutational analysis of EcoRII functional domains reveals evolutionary links between restriction enzymes, *FEBS Lett. 580*, 1665−1671.
30. Mucke, M., Pingoud, V., Grelle, G., Kraft, R., Kruger, D. H., and Reuter, M. (2002) Asymmetric photocross-linking pattern of restriction endonuclease EcoRII to the DNA recognition sequence, *J. Biol. Chem. 277*, 14288−14293.
31. Mucke, M., Grelle, G., Behlke, J., Kraft, R., Kruger, D. H., and Reuter, M. (2002) EcoRII: A restriction enzyme evolving recombination functions? *EMBO J. 21*, 5262−5268.
32. Alting-Mees, M. A., and Short, J. M. (1989) pBluescript II: Gene mapping vectors, *Nucleic Acids Res. 17*, 9494.
33. Kaus-Drobek, M., Czapinska, H., Sokolowska, M., Tamulaitis, G., Szczepanowski, R. H., Urbanke, C., Siksnys, V., and Bochtler, M. (2007) Restriction endonuclease MvaI is a monomer that recognizes its target sequence asymmetrically, *Nucleic Acids Res. 35*, 2035−2046.
34. Shlyakhtenko, L. S., Gall, A. A., Filonov, A., Cerovac, Z., Lushnikov, A., and Lyubchenko, Y. L. (2003) Silatrane-based

surface chemistry for immobilization of DNA, protein-DNA complexes and other biological materials, *Ultramicroscopy 97*, 279−287.

35. Henderson, R. M., Schneider, S., Li, Q., Hornby, D., White, S. J., and Oberleithner, H. (1996) Imaging ROMK1 inwardly rectifying ATP-sensitive K^+ channel protein using atomic force microscopy, *Proc. Natl. Acad. Sci. U.S.A. 93*, 8756−8760.
36. Livshits, M. A., Amosova, O. A., and Lyubchenko, Y. L. (1990) Flexibility difference between double-stranded RNA and DNA as revealed by gel electrophoresis, *J. Biomol. Struct. Dyn. 7*, 1237−1249.
37. Embleton, M. L., Vologodskii, A. V., and Halford, S. E. (2004) Dynamics of DNA loop capture by the SfiI restriction endonuclease on supercoiled and relaxed DNA, *J. Mol. Biol. 339*, 53−66.
38. Zhang, Y., McEwen, A. E., Crothers, D. M., and Levene, S. D. (2006) Statistical-mechanical theory of DNA looping, *Biophys. J. 90*, 1903−1912.
39. Du, Q., Smith, C., Shiffeldrim, N., Vologodskaia, M., and Vologodskii, A. (2005) Cyclization of short DNA fragments and bending fluctuations of the double helix, *Proc. Natl. Acad. Sci. U.S.A. 102*, 5397−5402.
40. Czapla, L., Swigon, D., and Olson, W. K. (2006) Sequence-Dependent Effects in the Cyclization of Short DNA, *J. Chem. Theory Comput. 2*, 685−695.
41. Anselmi, C., De Santis, P., Paparcone, R., Savino, M., and Scipioni, A. (2002) From the sequence to the superstructural properties of DNAs, *Biophys. Chem. 95*, 23−47.
42. Cloutier, T. E., and Widom, J. (2004) Spontaneous sharp bending of double-stranded DNA, *Mol. Cell 14*, 355−362.
43. Cloutier, T. E., and Widom, J. (2005) DNA twisting flexibility and the formation of sharply looped protein-DNA complexes, *Proc. Natl. Acad. Sci. U.S.A. 102*, 3645−3650.
44. Shlyakhtenko, L. S., Chernov, B. K., Lyubchenko, Y. L., and Zhurkin, V. B. (1990) Influence of temperature and ionic strength on electrophoretic mobility of synthetic DNA fragments, *Mol. Biol. (English Translation) 24*, 66−81.
45. Cherepanov, P., Surratt, D., Toelen, J., Pluymers, W., Griffith, J., De Clercq, E., and Debyser, Z. (1999) Activity of recombinant HIV-1 integrase on mini-HIV DNA, *Nucleic Acids Res. 27*, 2202−2210.
46. Halford, S. E., and Marko, J. F. (2004) How do site-specific DNA-binding proteins find their targets? *Nucleic Acids Res. 32*, 3040−3052.
47. Crampton, N., Yokokawa, M., Dryden, D. T., Edwardson, J. M., Rao, D. N., Takeyasu, K., Yoshimura, S. H., and Henderson, R. M. (2007) Fast-scan atomic force microscopy reveals that the type III restriction enzyme EcoP15I is capable of DNA translocation and looping, *Proc. Natl. Acad. Sci. U.S.A. 104*, 12755−12760.

BI701123U